AIAA JOURNAL
Vol. 34, No. 9, September 1996

Enriched Finite Elements for Regions with Multiple, Interacting Singular Fields

Stephane S. Pageau* and Sherrill B. Biggers Jr.†
Clemson University, Clemson, South Carolina 29634

Enriched two-dimensional finite elements are formulated for analysis of solids with interacting singular points. These elements contain both the order and the angular variation of all singular stress fields emanating from each singular point so that the possible interaction of stress states present in such regions is represented. The order and distribution of the singular fields are determined with a separate finite element eigenanalysis. These field characterizations and the subsequent enrichment are carried out numerically rather than analytically for ease of extension of the technique to complex geometries for which analytical solutions would be difficult to obtain. Generalized stress intensity factors as well as the stresses and displacements result directly from models incorporating enriched elements. Enriched-element models can be applied not only to crack problems but also to singular stress states not involving cracks and crack growth, and are thus more versatile than *J*-integral and virtual crack-closure techniques used for calculating energy release rates. In addition, the proper angular distribution of the displacement fields leading to each singular stress state is used in formulating the element, an advantage not shared by formulations such as the quarter-point elements. The advantages of using enriched elements containing information from interacting singular points are demonstrated with an example having two interacting singular points. This tensile groove specimen is modeled using these new elements as well as enriched elements that do not take interaction into consideration. Attention is given to modeling issues when using interactive enriched elements.

Introduction

THE difficulties that stress singularities present to conventional finite element analysis are well known. Many researchers,[1–5] have developed special elements that are especially suited for the high-stress gradients and stress levels present around crack tips. Both two- and three-dimensional special elements have been developed. Research in crack-tip elements is still active. The trend is to include more than just the square-root singular asymptotic stress field in the crack-tip element formulation.[6]

Many other geometries and/or material combinations, such as wedges and multimaterial junctions (see Fig. 1), lead to singular stress fields emanating from locations referred to as singular points. A method for quantification of these singular fields, particularly when multiple fields interact, is the objective of this paper. The *J*-integral and other energy-release-rate calculation techniques are not applicable to some of these geometries because the question is one of fracture initiation rather than defect propagation. Even though the research in this area is not as extensive as for crack tips with square-root singularities, some authors have addressed such problems.[7–9] In these papers, special elements that embed the leading order of the stress singularities at one node of the elements have been constructed. None of these elements, however, incorporate the asymptotic angular variation of the displacement or stress fields, nor do they incorporate nonleading orders of the stress singularities. More recently, Pageau and Biggers[10] created special elements in which all singular orders of the stress singularities as well as all asymptotic angular variations of the singular displacement fields are incorporated into the element formulation. These elements, which are directly extended from the formulation of Benzley,[4] are referred to as enriched elements. With these new elements, the singular point can be located outside of an element or can be coincident with a node. This approach gives more freedom to the placement of such elements in a finite element model than previously seen.

In Ref. 10, the elements created consider cases with only one singular point, such as those shown in the upper half of Fig. 1. If other singular points exist as shown in the lower half of Fig. 1, they are assumed not to interact with each other. Elements with interacting singular points have been developed.[11,12] However, these elements have the same limitations as those of Refs. 7–9. In addition, they have the interacting singular points coincident with two nodes of the elements, and, as a result, the size of such elements is directly linked to the distance between singular points.

This paper extends the formulation of Ref. 10 to incorporate multiple interacting singular points into the element formulation. All existing singular fields emanating from each singular point are incorporated. Also, these new enriched elements are developed such that the distance from one singular point to another is not constrained by the size of the elements. Formulation usage and validation is shown for a two-dimensional problem containing two interactive singularities.

Formulation

The current formulation follows directly from the authors' earlier paper[10] in which two- and three-dimensional enriched finite elements were developed for use in the neighborhood of a singular point. These elements can incorporate singular fields because of the presence of material and/or geometrical discontinuities in multimaterial wedges and junctions (see Fig. 1) as well as those due to cracks and disbonds. These enriched elements are unique in two ways: 1) They allow the use of numerically obtained asymptotic

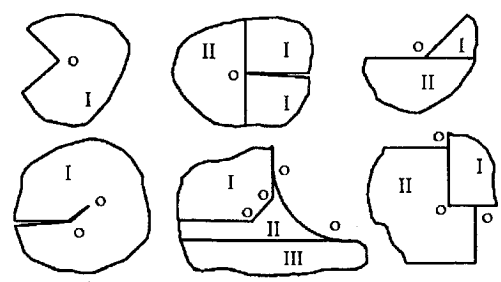

Fig. 1 Single and/or multimaterial wedges and junctions with or without interacting sigularities at *o*.

Received Dec. 31, 1994; revision received Dec. 30, 1995; accepted for publication Feb. 15, 1996.

*Ph.D. Student, Department of Mechanical Engineering; currently ABAQUS/Standard Developer, Hibbitt, Karlsson, and Sorensen, Inc., Pawtucket, RI 02860.

†Professor, Department of Mechanical Engineering. Associate Fellow AIAA.

singular displacement fields to enrich the elements; and 2) several layers of enriched elements can be placed around a singular point, thus enabling mesh refinement to be carried out as is normally done in finite element analyses. In Ref. 10, it is shown how accurate stress intensity factors and stresses can be obtained using enriched elements in conjunction with a mesh refinement technique. It is also shown there that using analytically obtained asymptotic displacement fields to obtain enriched elements, as has been done in the past for the specific case of cracks, does not provide an advantage over that of using finite elements enriched with numerical solutions for the asymptotic displacement fields. Also, because the displacement fields can be obtained easily for a variety of problems,[13–15] development of enriched elements using numerical fields is relatively simple and a broad range of applications can be found.

In this paper, the formulation developed in Ref. 10 is extended to construct enriched finite elements that carry singular field information from multiple singular points. This approach is attractive for regions where singular fields interact because of the close proximity of multiple singular points.

Two-Dimensional Enriched Elements Accounting for One Singular Point

As shown in Ref. 10, the enriched-element formulation of Benzley[4] for crack-tip elements can be extended to create enriched elements for sharp stress gradients because of other geometric or material discontinuities, as shown in Fig. 1. For the four-node element shown in Fig. 2, the displacement field around the singular point o is assumed in the form

$$u_i = \alpha_{i1} + \alpha_{i2}\zeta + \alpha_{i3}\delta + \alpha_{i4}\zeta\delta + \sum_{j=1}^{J} k_j Q_{ij}(r,\theta) \qquad (1)$$

where i represents the x and y directions, ζ and δ are natural coordinates of the element, J is the number of singular fields, α_{ij} are the unknown coefficients of the polynomial displacement approximation over the element, $Q_{ij}(r,\theta)$ is of the form $Q_{ij}(r,\theta) = r^{\lambda_j} f_{ij}(\theta)$ and represents the asymptotic displacement field (relative to the singular point) in the ith direction associated with the jth singular root λ_j, and k_j is the generalized stress intensity factor attributable to the displacement field $Q_{ij}(r,\theta)$. Because all of these fields are defined as displacements relative to a particular singular point, they introduce no stress or strain attributable to rigid body motion of the element. A four-node element is considered here only for simplicity. For elements containing more than four nodes, the polynomial part of Eq. (1) would contain additional quadratic, cubic, or other such terms.

One can solve for the unknown α_{ij} of Eq. (1) in terms of the nodal displacements as

$$u_i = \sum_{n=1}^{4} N_n \bar{u}_{in} + \sum_{j=1}^{J} k_j \left[Q_{ij}(r,\theta) - \sum_{n=1}^{4} N_n \bar{Q}_{ijn}(r,\theta) \right] \qquad (2)$$

where the N_n are the shape functions of a standard finite element, $\bar{u}_{in}$ and $\bar{Q}_{ijn}$ are, respectively, the displacement and the jth asymptotic displacement field values at node n for the displacement direction i. Elemental stiffness matrices for the enriched element created using the displacement assumption of Eq. (2) can be obtained in a straightforward manner as explained by Benzley.[4]

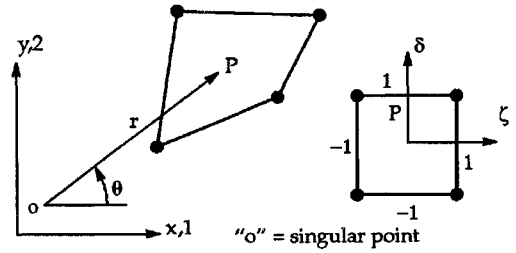

Fig. 2 Four-node enriched element in the global and natural coordinate systems.

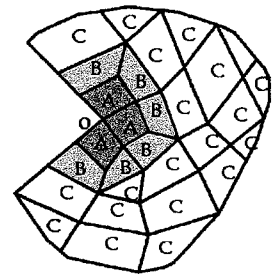

Fig. 3 Placement of elements: A) enriched, B) transition, and C) standard.

Geometry and displacement assumptions:

$$r = r_o\left(\frac{1+\xi}{2}\right)^{1/\lambda} \qquad \theta = \sum_{i=1}^{3} H_i\theta_i$$

$$H_1 = \tfrac{1}{2}(-\eta+\eta^2),\quad H_2 = 1-\eta^2,\quad H_3 = \tfrac{1}{2}(\eta+\eta^2)$$

$$\{\bar{u}_j\} = \left(\frac{r}{r_o}\right)^{\lambda_j}\{f_j(\theta)\} \quad \text{with} \quad \{f_j(\theta)\} = \left[\sum_{n=1}^{3} H_n \{\bar{u}_{jn}\}\right]$$

Nodal displacements for the j^{th} eigenvalue λ_j.

$\bar{u}_{rjn}$=radial displacement at node n relative to pt. o.

$\bar{u}_{\theta jn}$=tangential displacement at node n relative to pt. o.

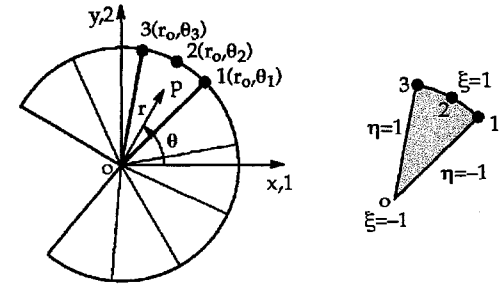

Fig. 4 Two-dimensional finite element model to obtain the order of the stress singularities λ_j and the angular variation of the displacements.

Benzley[4] also showed that transition elements are needed to join enriched elements to standard elements in a finite element model so that no displacement-field incompatibility will exist between enriched and standard elements. Considering Fig. 3, the transition elements (B) are placed between the enriched elements (A) and the standard elements (C). The displacement field of a transition element is given by the relation

$$u_i = \sum_{n=1}^{4} N_n \bar{u}_{in} + R(\zeta,\delta)\sum_{j=1}^{J} k_j \left[Q_{ij}(r,\theta) - \sum_{n=1}^{4} N_n \bar{Q}_{ijn}(r,\theta) \right] \qquad (3)$$

where $R(\zeta,\delta)$ is one along boundaries adjacent to enriched elements and zero along boundaries adjacent to standard elements. The variation of the function $R(\zeta,\delta)$ over the transition element can take various forms. For simplicity, the functions defined by Benzley[4] are used here.

The finite element formulation developed by the authors[13,14] can be used to produce the angular variation of the displacement field as well as the order of the stress singularity for a variety of problems in a simple manner. Figure 4 shows a typical finite element model that can be used to define the singular displacement field, illustrated in this case for a wedge geometry. Here the angular variation of the displacement field is determined using shape functions that are quadratic in θ across each element. The accuracy of the eigenanalysis is discussed in detail elsewhere.[13,14] In general, four-digit accuracy in the eigenvalues λ_j can be achieved with small models having on the order of 10–30 elements using low-order quadrature (3 Gauss points) for two-dimensional and quasi-three-dimensional models of isotropic and anisotropic materials. Angular distributions of displacements, the eigenvectors, were shown to have similar accuracy. Thus the computational effort involved in accurately characterizing the singular fields is quite small. In problems requiring a

true three-dimensional characterization,[15] the computational effort is much larger, though still quite reasonable compared to solution of the final models including the enriched elements.

The displacement shapes obtained previously[13,14] are in cylindrical coordinates, whereas the current formulation assumes that the functions Q_{ij} are given in a Cartesian coordinate system. Using the notation of Fig. 4, the displacement field relative to a singular point o is given over each element by

$$Q_{1j}(r,\theta) = r^{\lambda_j}\left[\left(\sum_{n=1}^{3} H_n \bar{u}_{rjn}\right)\cos(\theta) - \left(\sum_{n=1}^{3} H_n \bar{u}_{\theta jn}\right)\sin(\theta)\right] \tag{4}$$

$$Q_{2j}(r,\theta) = r^{\lambda_j}\left[\left(\sum_{n=1}^{3} H_n u_{rjn}\right)\sin(\theta) + \left(\sum_{n=1}^{3} H_n \bar{u}_{\theta jn}\right)\cos(\theta)\right] \tag{5}$$

where the subscripts 1 and 2 represent the x and y components of the displacements, respectively, for the jth order of stress singularity λ_j. The functions $Q_{ij}(r,\theta)$ are obtained from angular variations of displacements in the radial and tangential directions, r and θ, by making use of quadratic shape functions H_n at node n. The validity of Eqs. (4) and (5) is limited to angles within the angles defined by nodes 1 and 3 of each element.

In creating the elemental stiffness matrices, one needs the derivatives of the functions $Q_{ij}(r,\theta)$ with respect to the variables r and θ. Differentiation with respect to r is straightforward in view of Eqs. (4) and (5). Differentiation with respect to θ is also obtained analytically from Eqs. (4) and (5) and the shape functions H_i shown in Fig. 4. Values of these derivatives of the displacement fields, and therefore of the stresses and strains, can be evaluated at any point in the element. Each elemental stiffness matrix can be constructed easily as described previously.[4] However, the complexity of the integrands in the stiffness matrices requires high-order quadrature for accuracy. An investigation of the order of integration led to the conclusion that a 16 × 16 point integration scheme is needed in most cases so that good accuracy can be achieved in models with a reasonable number of enriched elements.[10] Note that, for simplicity, Eqs. (4) and (5) consider only two-dimensional elements with in-plane deformation only. The formulation of the functions $Q_{ij}(r,\theta)$ and their derivatives for two-dimensional geometries with three-dimensional displacements can be found elsewhere.[10]

Two-Dimensional Enriched Elements Accounting for Multiple Singular Points

Figure 5 represents a four-node element located in a region where M singular fields interact. The displacement at point P is assumed to be of the form

$$u_i = \alpha_{i1} + \alpha_{i2}\zeta + \alpha_{i3}\delta + \alpha_{i4}\zeta\delta + \sum_{m=1}^{M}\sum_{j=1}^{J} k_{jm} Q_{ijm}(r_m,\theta_m) \tag{6}$$

where the subscript m represent the mth singular point and all other quantities are as defined earlier. The singular-fields functions

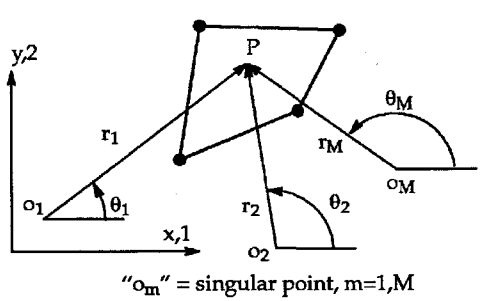

Fig. 5 Four-node enriched element in the global coordinate system where M singular points interact.

$Q_{ijm}(r_m,\theta_m)$ and their derivatives are obtained numerically as explained earlier, with the difference being that separate polar coordinate systems are considered for each of the singular points. Solving for the unknown coefficients α_{ij} of Eq. (6) in terms of the nodal displacements, one obtains

$$u_i = \sum_{n=1}^{4} N_n \bar{u}_{in} + \sum_{m=1}^{M}\sum_{j=1}^{J} k_{jm}\left[Q_{ijm}(r_m,\theta_m) - \sum_{n=1}^{4} N_n \bar{Q}_{ijmn}(r_m,\theta_m)\right] \tag{7}$$

The singular points are either outside of the enriched element shown in Fig. 5, or coincide with one or more nodes of the elements. Straightforward extension of Eq. (3) also is possible to create transition elements containing information from multiple singular fields as

$$u_i = \sum_{n=1}^{4} N_n \bar{u}_{in} + \sum_{m=1}^{M} R_m(\zeta,\delta) \times \sum_{j=1}^{J} k_{jm}\left[Q_{ijm}(r_m,\theta_m) - \sum_{n=1}^{4} N_n \bar{Q}_{ijmn}(r_m,\theta_m)\right] \tag{8}$$

In general, a transition element may be required between standard elements and an element enriched with the pth singularity but not with the qth one, which explains the subscript m on the function $R_m(\zeta,\delta)$. This feature is discussed in the following section for specific cases.

Results

This section presents an application of the above formulation to a two-dimensional test case of interest. The mesh refinement technique described previously[10] is used here, and the details related to the placement of enriched and transition elements in regions where more than one singular field is present are addressed. The test-case geometry is that of a tensile specimen with a rectangular edge groove. When the groove is of finite width, there are two singular points that can interact. The degree of interaction is investigated using enriched elements with multiple singular points and using enriched elements with only one singular point. All elements created here (i.e., types A and B) have been incorporated into the finite element commercial code ABAQUS[16] through the user-defined capability of the software. Elements of type C are the standard bilinear continuum elements in the ABAQUS element library.

Figure 6 depicts half of a specimen containing a groove of length a and total width $2h$. This specimen is composed of only one material

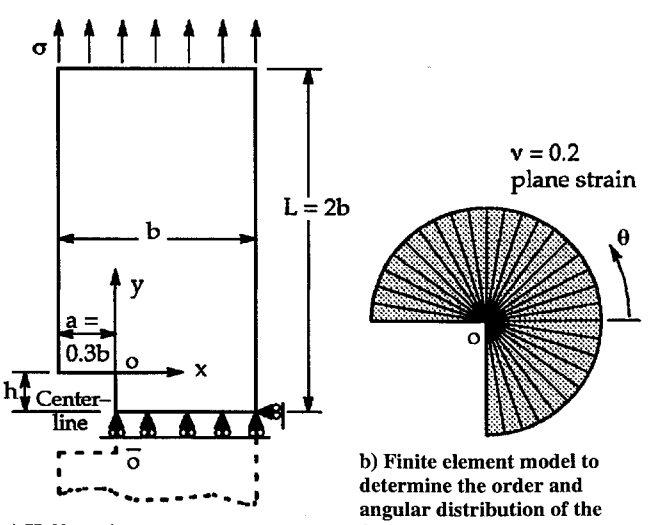

Fig. 6 Rectangular groove specimen with two interacting singular-points o and $\bar{o}$.

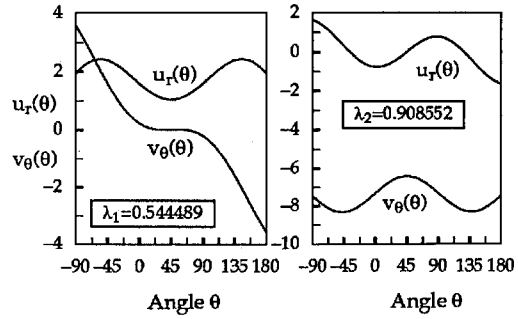

Fig. 7 Displacement fields for the two singular eigenvalues, 30-element model, Fig. 6b.

with properties and loading conditions indicated. Every dimension but h is fixed in this study. Also shown is a 30-element model used to characterize the asymptotic singular fields present around point o. A numerical value for the radius r_o (see Fig. 4) is not shown or needed because the formulation is in terms of the dimensionless quantity r/r_o ranging from 0 to 1. The formulation developed previously[13,14] has been used to obtain the results, which are shown in Fig. 7 for the two λ leading to singular stresses. The angular distributions of the displacements are valid at any value of r/r_o. These displacement functions are necessary for developing enriched elements with one singular point as well as enriched elements with two singular points. The functions $Q_{ij}(r, \theta)$ have been normalized such that the angular variations of the fields lead to $\sigma_{\theta\theta}(\theta = 0) = kr^{\lambda_i - 1}$.

Development of stiffness matrices for elements having interactive singularities follows the same approach presented previously,[10] modified to account for multiple singular points as discussed in the preceding section. To obtain stiffness matrices that contain information from both the singular point o and its symmetric point $\bar{o}$ (see Fig. 6), one has to consider the entire specimen, even if there is an obvious symmetry as is the case for this problem. In other words, the net interactive effect at point o of the two singular fields cannot be represented simply as the mirror image of one field about the line of symmetry. If this approach were taken, the interactive effect would be unaccounted for. Rather, the net effect at point o includes the two fields associated directly with that point plus the smaller effects of the two fields associated with the adjacent point $\bar{o}$. As a result, two generalized stress intensity factors k_1 and k_2 associated with each singular point are obtained. This represents four unknowns for the problem considered here, in addition to the unknown nodal displacements. In this case, because of the symmetry of geometry and loading about the centerline, the two k_1 values will be identical, and the two k_2 values will be equal and of opposite sign.

Figure 8 shows three possible configurations for placement of enriched elements around point o. Figure 8a shows an enriched region composed of enriched elements that only contain asymptotic information related to the singular point o. This constitutes the approach used in most previous studies in which the proximity of multiple singular points is not accounted for. This enriched region is surrounded by one layer of transition elements, the rest of the upper half of the specimen being modeled using conventional four-node standard elements. If one assumes that the asymptotic fields have a roughly uniform radial influence around point o (i.e., point o is assumed to be at equal distance from each corner of the box as shown in Fig. 8a), the size of the enriched region must be such that $c \leq h$. This limits the sizes of enriched regions that can be used in assessing solution convergence. On the other hand, Figs. 8b and 8c represent configurations in which the enriched region size is not limited by the groove half-width h. However, here the darkly shaded regions contain enriched elements that must possess information from both singular points present. The lightly shaded region cannot contain information from the symmetric point $\bar{o}$ because the angular variation of its singular fields does not extend beyond the end face of the groove. For cases where c is much less than h, the choice of Fig. 8b is not very reasonable because it would assume that the influence of the singular fields emanating from point o is much greater below the line $y = 0$ (see Fig. 6) than above that same line, which is of course not known a priori. In such a case, the scheme shown in Fig. 8a is

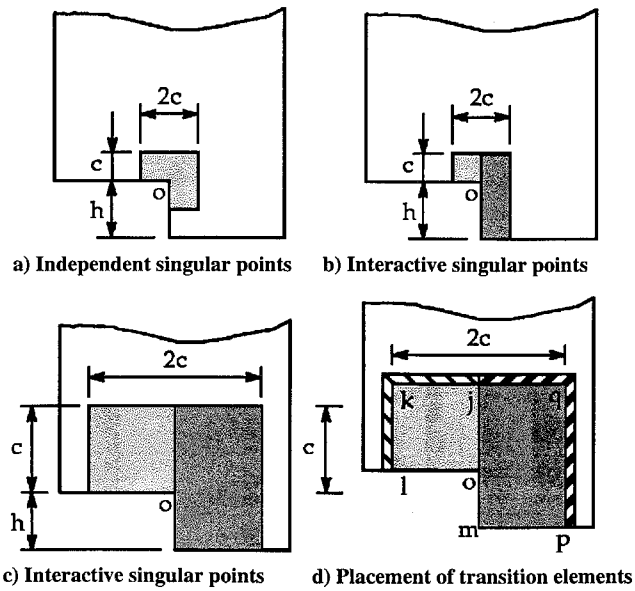

Fig. 8 Possible arrangements of enriched and transition elements for the groove specimen of Fig. 6a.

more advisable. However, when c is only slightly less than h, the approach shown in Fig. 8b is legitimate. The model in Fig. 8c, where $c > h$, illustrates the case when the influence of both singular points must be considered.

As explained earlier, when enriched elements containing information emanating from more than one singular point are used, the transition elements must also account for the presence of multiple singular points. In Fig. 8d, the lightly cross-hatched border (lkj) around the lightly shaded region schematically represents one layer of transition elements containing information about the point o only. The darker cross-hatched border (jqp) represents one layer of transition elements containing information from both singular points. For these transition elements, the zeroing functions used in Eq. (8) are such that $R_1(\zeta, \delta) = R_2(\zeta, \delta)$. This is the simplest possible combination of enriched and transition elements for cases where multi-singular-point enriched elements are used. With such a choice, a slight displacement incompatibility exists between element edges joining along the line oj shown in Fig. 8d. Of course, no nodal displacement incompatibilities exist, and the element edge incompatibilities tend to zero with mesh refinement. Furthermore, the singular fields emanating from point o are such that σ_x and τ_{xy} are zero along this line in this problem. Therefore, stress continuity is automatically satisfied across each enriched region separated by the line oj.

Moreover, the formulation in Eq. (8) could be used to completely eliminate the displacement incompatibility along line oj. An additional band of elements along line oj within the region ($jmpq$) could be defined in which $R_2(\zeta, \delta)$ varies from 0 to 1 along ζ and $R_1(\zeta, \delta) = 1$, in effect creating a smooth transition between the region affected by only one singular point and the region affected by both singular points. Thus Eq. (8) enables transition between adjacent enriched regions as well as between enriched- and conventional-element regions. Additional investigations could be carried out using this and other transition schemes.

A number of different finite element models have been constructed for different values of h. Figure 9 shows values of generalized stress intensity factors for different values of h, and different sizes of enriched regions. The enriched regions chosen are represented schematically in Figs. 8b and 8c with the arrangement of transition elements shown in Fig. 8d. A trend toward convergence is seen in all cases but it is much more rapid for k_1 than for k_2. Results for the smallest region ($c = 0.1b/\pi$) showed slow or no convergence, indicating undersizing. Therefore, to maintain clarity, these data are not included in Fig. 9. The values of the generalized stress intensity factor k_1 predicted with models using $c = 0.3b/\pi$ and $c = 0.6b/\pi$ differ by less than 1% for all groove half-widths.

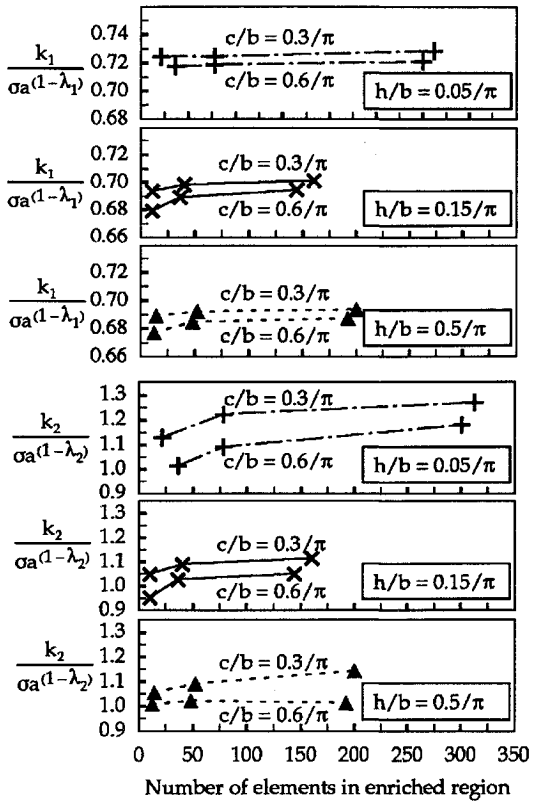

Fig. 9 Generalized stress intensity factors k_1 and k_2 for different sizes of enriched regions, using interactive enrichment.

The relatively poor accuracy of k_2 vs k_1 is attributable to the dominance of the first singular field in the evaluation of the stresses.

For each value h, choosing the best size for the enriched region on the basis of convergence of the generalized stress intensity factors is not easy. However, by also considering reduction of interelement stress jumps across enriched-element boundaries and from transition to standard elements (as discussed previously[10]), $c = 0.6b/\pi$ was chosen as the most appropriate of the three models considered for all values of h. Models with the smallest enriched region ($c = 0.1b/\pi$) exhibited large stress jumps, again indicating that the enriched region is clearly undersized. For all other cases investigated, the difference in stresses along the line $y = 0$ obtained with $c = 0.3b/\pi$ and $c = 0.6b/\pi$ is less than 1.5%.

Figure 10 shows plots of stresses along the line $y = 0$, from the singular point o to the edge of the enriched region using $c = 0.6b/\pi$, the most refined model, and interactive enrichment. The stresses shown here are those obtained at nodes without averaging between elements. It is obvious that the interelement stress jumps are extremely small in the enriched models, whereas the same cannot be said for the conventional models. Both methods produce the same stresses away from the source of singularity, indicating that the singularity has dissipated at the right-hand side of the enriched region (right-hand side of the graphs). Of course, use of only conventional elements is not effective for this class of problems as indicated by the roughness of the dashed lines near $x = 0$. This poor performance of standard elements is expected because they are formulated assuming a symmetric stress tensor and, therefore, cannot explicitly admit singularities such as those that occur here. Along these lines,[10] the zero tractions on the free surfaces intersecting the singular points are predicted extremely accurately with enriched elements but not at all accurately with standard elements for the reason stated above.

A summary of the stresses normal to the line $y = 0$ computed for the three groove widths is shown in Fig. 11. The data are taken from the σ_y plots with interactive enrichment in Fig. 10. Here the quantity $\sigma_y\sqrt{x}$ along the line $y = 0$ is plotted as a function of the distance $x/(b-a)$ from the grove edge to the right-hand side of the specimen. The curve obtained for $h = 0$ has been taken from the edge-crack tensile specimen study discussed previously.[10] Figure 11

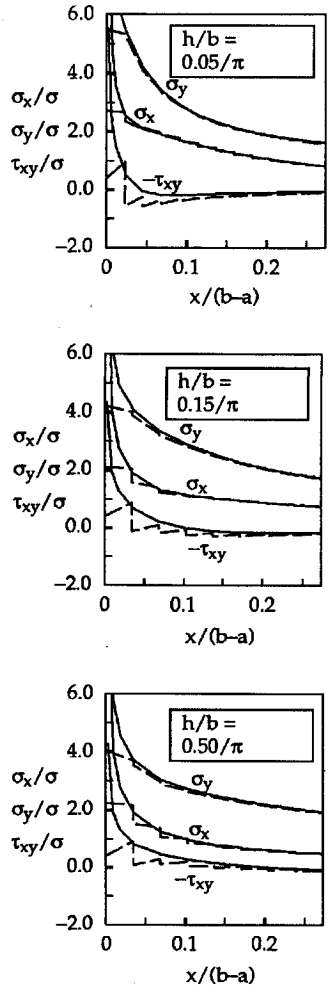

Fig. 10 Stresses along the x-axis (Fig. 6) using interactive enrichment with $c/b = 0.6/\pi$ (solid lines) and using no enrichment (dashed lines).

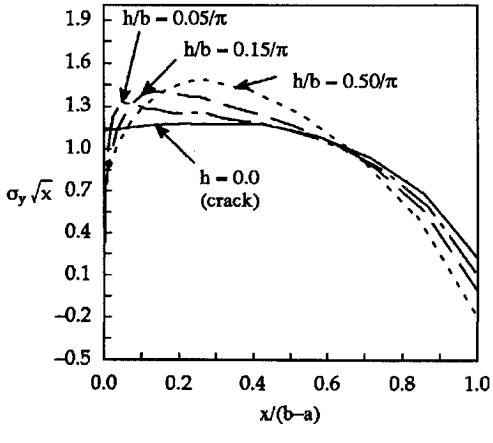

Fig. 11 Comparative plot of normal stress σ_y along the x axis, as a function of groove width h.

shows that as h diminishes, the case of the crack is recovered. Such curves could not be generated with sufficient precision using standard elements because limiting values as x approached zero would require extremely small conventional elements. Also, the obvious interaction of fields as h becomes very small would invalidate results with noninteractive enriched elements.

The difference in independent enrichment (the approach of Fig. 8a) vs interactive (Fig. 8b) is illustrated in Figs. 12 and 13. In these figures, the solid lines correspond to data obtained using both singular points, and the dashed lines correspond to use of only one

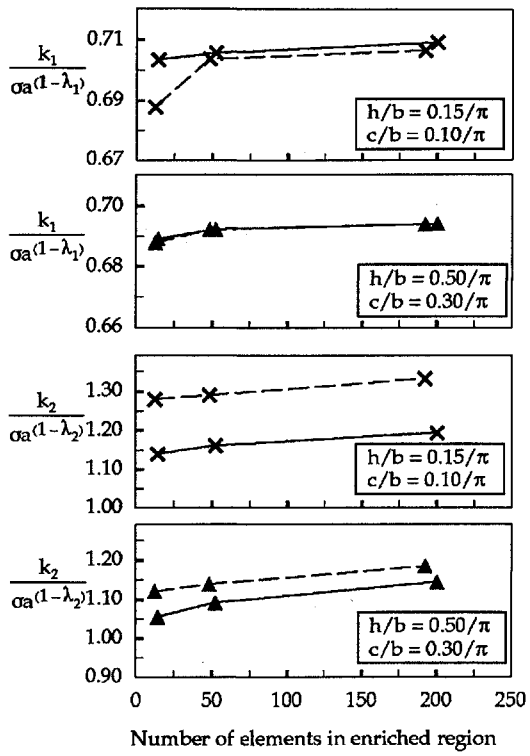

Fig. 12 Effect of considering interactive sigular points on generalized stress intensity factors k_1 and k_2: — —, independent singular points and ——, interactive singular points.

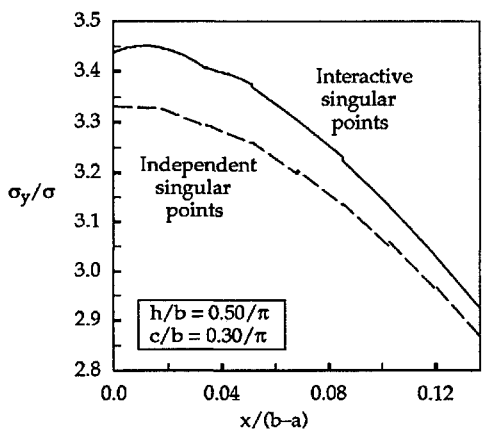

Fig. 13 Effect of considering interactive singular points on the normal stress σ_y.

singular point. For each value of groove width, the models included the largest-size enriched region for which the assumption of noninteracting fields was reasonable. Recall that the best results found for all values of h investigated occurred with $c = 0.6b/\pi$ (Fig. 8c). This case cannot be evaluated with the noninteractive approach of Fig. 8a because the enriched regions overlap and therefore must be considered to interact. Therefore, the comparative results are necessarily obtained from models with undersized enriched regions. The models with interacting fields maintained the same size of the enriched region except that the region was extended vertically to the centerline, as shown in Fig. 8b. No comparison between the two approaches is shown for the narrowest groove width, $h = 0.05b/\pi$, because enriched regions small enough to be independent ($c < 0.05/\pi$) would be grossly undersized. In other words, with $h = 0.05b/\pi$ the two singular points are so close that interaction of the singular fields is an essential consideration. With the medium-width groove, $h = 0.15b/\pi$, more rapid convergence is obtained for k_1 using interactive singular points, although the converged values of k_1 differ by only 0.4%. With the widest groove, $h = 0.5b/\pi$, the singular points are far enough removed so that interaction is negligible with respect to k_1 and the two approaches give the same results. Results for k_2 with $h = 0.15b/\pi$ indicate a lack of convergence when independent fields are considered and more rapid convergence with $h = 0.5b/\pi$ when interaction is considered. The generally slower convergence of k_2 compared to k_1 is, here again, attributable to the dominance of the first singular field.

Stress values and distributions are somewhat more sensitive to consideration of the independence or interaction of fields. For example, consider the data shown in Fig. 13 corresponding to the widest groove, $h = 0.5b/\pi$ (for which essentially no interactive effect exists with respect to k_1), with the largest enriched region, $c = 0.3b/\pi$, for which independent fields can be modeled. For the models using single-point enrichment, there is one row of transition elements immediately above the centerline. In addition, consider the σ_y stresses along the centerline, a location remote from the singular points in this case. With single-point enrichment, the influence of the singular point is assumed to become zero at the centerline whereas with interacting enrichment, the effects of both singular points are felt along this line. Even though the k_1 values were essentially identical between the two approaches for this case, the stress σ_y is about 3% higher when interaction of the singular points is accounted for. Larger differences exist when the groove is narrower and consideration of interaction becomes more important, and in some cases a necessity for convergence and accuracy.

Conclusions

Solutions for the order and the angular variations of singular displacement fields determined numerically from a finite element eigenanalysis can be used to create enriched two-dimensional or three-dimensional finite elements for analysis of solids with material and/or geometric discontinuities. These elements can be placed in regions where one or more singular points are present. For the latter case, interaction between singular points is properly considered when formulating such elements. For example, with two identical adjacent singular points, a number of two-dimensional models with or without interaction of the singular fields are used to assess the performance of such elements. With reasonably close singular points, convergence on generalized stress intensity factors was slower or nonexistent if interaction of the fields was not accounted for. Even considering interaction, an improper choice of the enriched region led to lack of convergence on k_i and large differences in stresses between adjacent elements. Even in geometries not exhibiting significant field interaction with respect to k_1, stress values remote from the singular points can be significantly affected if field interaction is neglected. Furthermore, in the case of a specimen with an increasingly narrow rectangular groove, the stress distributions correctly approach the limiting case of a crack in which the interacting singular points become coincident. Accurate solutions for such cases with close singular fields are only possible if interaction is considered in the element formulation.

Acknowledgments

The authors acknowledge the support of NASA Langley Research Center through Grant NAG-1-1411, J. H. Starnes Jr., monitor.

References

[1]Barsoum, R. S., "Quarter-Point Elements in Fracture Mechanics," *Recent Advances in Engineering Sciences, Proceedings of the 14th Annual Meeting* (Bethlehem, PA), 1977, pp. 925–932.

[2]Tracey, D. M., "Three-Dimensional Elastic Singularity Elements for Evaluation of Stress-Intensity Factor Along an Arbitrary Crack Front," *International Journal of Fracture*, Vol. 9, No. 3, 1973, pp. 340–343.

[3]Hilton, P. D., Kiefer, B. V., and Sih, G. C., "Specialized Finite Element Procedures for Three-Dimensional Crack Problems," *Numerical Methods in Fracture Mechanics*, Vol. 10, 1978, pp. 485–496.

[4]Benzley, S. E., "Representation of Singularities in the Isoparametric Finite Elements," *International Journal for Numerical Methods in Engineering*, Vol. 8, No. 3, 1974, pp. 537–545.

[5]Pian, T. H. H., and Moriya, K., "Three-Dimensional Crack Element by Assumed Stress Hybrid Element," *Recent Advances in Engineering Sciences, Proceedings of the 14th Annual Meeting* (Bethlehem, PA), 1977, pp. 913–917.

[6]Kuna, M., and Zwicke, M., "A Mixed Hybrid Finite Element for Three-Dimensional Elastic Crack Analysis," *International Journal of Fracture*, Vol. 45, No. 1, 1990, pp. 65–79.

[7]Tracey, D. M., and Cook, T. S., "Analysis of Power Type Singularities Using Finite Elements," *International Journal for Numerical Methods in Engineering*, Vol. 11, No. 8, 1977, pp. 1225–1233.

[8]Lim, W. K., and Kim, S. C., "Further Study to Obtain a Variable Power Singularity Using Quadratic Isoparametric Elements," *Engineering Fracture Mechanics*, Vol. 47, No. 2, 1994, pp. 223–228.

[9]Dutta, B. K., "A Six-Noded Element for Analysing Power-Type Singularities Under Thermal Loads," *International Journal for Numerical Methods in Engineering*, Vol. 36, No. 13, 1993, pp. 2287–2303.

[10]Pageau, S. S., and Biggers, S. B., Jr., "Enrichment of Finite Elements with Numerical Solutions for the Singular Stress Field," *International Journal for Numerical Methods in Engineering* (submitted for publication).

[11]Dutta, B. K., Maiti, S. K., and Kakodkar, A., "Development and Applications of Two Singular Points Finite Elements," *International Journal for Numerical Methods in Engineering*, Vol. 28, No. 6, 1989, pp. 1449–1460.

[12]Dutta, B. K., Maiti, S. K., and Kakodkar, A., "On the Use of One and Two Points Singularity Elements in the Analysis of Kinked Cracks," *International Journal for Numerical Methods in Engineering*, Vol. 29, No. 7, 1990, pp. 1487–1499.

[13]Pageau, S. S., Joseph, P. F., and Biggers, S. B., Jr., "Finite Element Analysis of Anisotropic Materials with Singular Inplane Stress Fields," *International Journal of Solids and Structures*, Vol. 32, No. 5, 1995 pp. 571–591.

[14]Pageau, S. S., and Biggers, S. B., Jr., "A Finite Element Approach to Three-Dimensional Singular Stress States in Anisotropic Multi-Material Wedges and Junctions," *International Journal of Solids and Structures*, Vol. 33, No. 1, 1995, pp. 33–47.

[15]Pageau, S. S., and Biggers, S. B., Jr., "Finite Element of Free-Edge Singular Stress Fields in Anisotropic Materials," *International Journal for Numerical Methods in Engineering*, Vol. 38, No. 13, 1995, pp. 2225–2239.

[16]Anon., *ABAQUS Theory and User's Manuals*, ver. 5.3, Hibbit, Karlsson, and Sorensen, Inc., Pawtucket, RI, 1993.